CHAPTER IV

Intensity-invariance of odor quality is optimized by the antennal lobe network in the honeybee

ABSTRACT

The dependence of perceived odor quality on odorant concentration has been investigated in several behavioral studies, but little is known about the underlying neural mechanisms performed by the primary olfactory center, the vertebrates' olfactory bulb or its insect analog, the antennal lobe (AL). To investigate strategies involved in olfactory processing we simultaneously measured the receptor neuron input and projection neuron output responses of identified glomeruli to odors spanning 7 log units of concentration using calcium imaging in the honeybee AL. We found that increasing concentration led to stronger responses and more glomeruli being excited over the AL. Stimulus intensity may thus be encoded as overall excitation. Dose-response functions of the most-responsive glomeruli were sigmoidal and comprised dynamic ranges of 3-4 log units for both input and output neurons. Some glomeruli had steeper response functions than others, leading to shifts in the sequence of most-activated glomeruli over the concentration range. Glomeruli with weak and intermediate responses in the input had reduced responses in the output, leading to lower numbers of activated glomeruli and contrast-enhanced odor representations. Additionally, the relative responses of the most-responsive glomeruli are changed in an odor-specific manner, in some cases even reducing the response of the strongest glomerulus. As a result, different odors can be separated to much lower concentrations in the output neurons than in the input. Taken together, the AL network optimizes odor representation by increasing reliable odor representations at lower concentrations, improving concentration-invariance for odor quality detection, and reliably representing odor-intensity in its overall excitation.

INTRODUCTION

Animals have to recognize odors which occur in plumes at a variety of concentrations. An important task for the olfactory system is therefore to extract odor quality independently from its occurring intensity. The first brain area to process olfactory information is the

olfactory bulb and its insect analogue, the antennal lobe (AL). Both are subdivided into functional processing units, the olfactory glomeruli. The hypothesis that odors are represented by specific spatio-temporal combinatorial patterns of activated glomeruli (Hildebrand and Shepherd 1997) has recently been confirmed by several optical recording studies in vertebrates (Friedrich and Korsching 1997; Rubin and Katz 1999; Uchida et al. 2000; Fuss and Korsching 2001; Meister and Bonhoeffer 2001; Wachowiak and Cohen 2001; Fried et al. 2002; Spors and Grinvald 2002; Wachowiak et al. 2002) and invertebrates (Joerges et al. 1997; Galizia et al. 1999b; Sachse et al. 1999). The afferent input to a particular glomerulus is determined by the response profile of a specific RN type, since each RN expresses only one olfactory receptor and RNs expressing the same receptor converge onto single glomeruli in vertebrates (Ressler et al. 1994; Vassar et al. 1994; Mombaerts et al. 1996) and in *Drosophila* (Gao et al. 2000; Vosshall et al. 2000).

Yet, the neural mechanisms underlying the processing of odor quality and intensity are poorly understood. Physiological measurements of olfactory receptor neurons (RNs) of vertebrates as well as of invertebrates have reported that RNs have broadly-tuned molecular response profiles (Sicard and Holley 1984; Sato et al. 1994; Duchamp-Viret et al. 1999; Malnic et al. 1999) to ensure a detection of the vast array of odorant molecules. With increasing odor concentrations these response profiles become broader and less specific (Sato et al. 1994; Malnic et al. 1999), leading to changes of the odor representations in the brain. The olfactory system may therefore sharpen the broader RN responses to realize a concentration-invariant detection of odor quality. Indeed, such mechanisms have been described in vertebrates and invertebrates (Yokoi et al. 1995; Sachse and Galizia 2002).

We used calcium imaging to investigate the odor representation in the AL of the honeybee, *Apis mellifera*, to stimuli over concentration ranges spanning 8 log units. In the honeybee, 60,000 RNs are distributed on each antenna (Esslen and Kaissling 1976) and project to 160 glomeruli of the AL, which can be individually identified based on their shapes and relative positions (Flanagan and Mercer 1989; Galizia et al. 1999a). Within the AL the afferent input is processed by about 4000 local interneurons (LNs) (Witthöft 1967) and then relayed via three distinct antenno-cerebralis tracts (ACTs) to higher-order brain centers by 800 projection neurons (PNs, corresponding to vertebrate mitral cells) (Hammer 1997). Using calcium imaging the afferent input to the AL can be estimated by bath-application of calcium-green AM (Galizia et al. 1998), whereas the output of the olfactory glomeruli is accessible by selectively staining PNs with fura-dextran (Sachse and Galizia 2002). By combining these two approaches in one animal we can directly measure how the cellular network of the AL shapes the representation of odors. We show that the AL network modulates and optimizes the afferent input by contrast-enhancing the odor representations, improving discrimination of odor identity at low concentrations, and increasing concentration-invariance of odor-evoked response patterns.

MATERIAL AND METHODS

Preparation and dye loading

Adult worker honeybees (*Apis mellifera*) were caught from different hives in the morning. Bees were anesthetized by cooling, fixed in a Plexiglas stage using dental wax and fed with sucrose solution. A small window was cut into the cuticle on the dorsal side of the head, and glands and tracheae were carefully removed. A glass electrode, which was coated with crystals of the calcium-sensitive dye fura-dextran (potassium salt, 10,000 MW, Molecular probes, Eugene, OR), dissolved in 2% bovine serum albumin solution, was inserted into the deutocerebrum lateral to the α-lobe, aiming for the projection neurons (PNs) of the lateral antenno-cerebralis tract (l-ACT). We have already shown that this dye application method is specific and effective for fura-dextran (3,000 MW) in a previous study (Sachse and Galizia 2002). After the dye application, the brain was rinsed with Ringer solution (130 mM NaCl, 6 mM KCl, 4 mM $MgCl_2$, 5 mM $CaCl_2$, 160 mM sucrose, 25 mM glucose, 10 mM HEPES, pH 6.7, 500 mOsmol; all chemicals from Sigma) several times to remove extracellular dye. The cut piece of cuticle was repositioned to prevent the brain from drying out. After 3 h of staining the antennae were immobilized with two silicone components (Kwik-Sil TM, WPI) at their scapus and covered with a coverslip while leaving the brain accessible for a water objective. Afterwards a big window was cut into the cuticle to expose the whole brain and again remaining glands and tracheae were removed. Only if the PNs were successfully stained with fura-dextran, which was visible by a strong staining of the l-ACT somata under the fluorescence microscope, did we stain the brain with the second calcium-sensitive dye. 50 µg of dye, calcium green 2-AM (Molecular Probes, Eugene, OR) was first dissolved in 50 µl Pluronic in dimethylsuphoxide (DMSO) and then diluted in 950 µl Ringer solution. The whole brain was exposed and stained by bath-application. After 1 h of staining the brain was washed with Ringer solution in order to remove excess dye and the abdomen was cut.

Odor stimulation

The animal's antennae were exposed to a constant clean air stream. The odor-loaden air was introduced into the continuous air stream to avoid mechanical stimulation. The stimulus timing was computer controlled and lasted for 1 s. Odors used were 1-hexanol, 1-octanol and 1-nonanol (all from Sigma-Aldrich, Deisenhofen). Odors were dissolved in mineral oil. Dilution was adjusted to equal effective vapor pressure for the different odorants. The control stimulus was a glass cartridge plus filter paper with mineral oil. For each odor, 6 µl were placed on filter paper in glass cartridges. Odor concentration was varied by using different dilutions, resulting in different effective amounts on the filter paper (from 10^{-7} to 10^{0} for all odors). Not all odors with all concentration levels were used in all animals. Therefore

the number of animals for each odor differs. Generally, the experiment started with the presentation of one odor at low concentration followed by higher concentrations of the same odor with the control stimulus in between. The entire stimulus sequence comprising all concentrations of one odor was repeated in each animal.

Imaging

Imaging was done using a T.I.L.L. Photonics imaging system (Martinsried, Germany). Monochromatic excitation light alternated between 340, 380 and 475 nm, dicroic: LP 505 nm, emission: LP 515. These filter settings allowed us to measure semi-simultaneously the two calcium-sensitive dyes, calcium green 2-AM and fura-dextran. Measurements were made with an upright microscope (Olympus BX 50WI), using a 20 x water-immersion objective (NA 0.5). Pixel image size was 2.4 x 2.4 µm, obtained by 2 x 2 binning on chip. For each stimulus a series of 60 triple frames was taken with frequencies of 6 Hz. Light was shut off between frames. The stimulus was given at frame 12. The interstimulus interval was 40 s, thus the bee was not exposed to light for about 30 s between measurements.

The number of bees differed depending on the staining procedure. Clear and consistent PN responses were registered in 16 of 65 bees tested. Since cell loading with calcium green was only successful on average in 1 of 2 bees, we measured compound signals in only about half of the bees (i.e. n=7), which showed PN responses. Moreover, reliable calcium green signals could only be measured for about 30 minutes, whereas the amplitude of the fura signals remained unchanged for about 1.5 hours. When using calcium green alone calcium responses could be measured for about 1.5 hours as well (data not shown). Thus, the calcium green dye is probably damaged by the UV light after several measurements. However, during the first 30 minutes, both dyes could be measured separately.

Data processing and analysis

All analyses were done using a custom software written in IDL (Research Systems, CO). The raw data were median-filtered for shot noise reduction (filter size 3 pixels in two spatial and one temporal dimension) and were corrected for scattered light by calculating an unsharp image with a radius of 50 µm and subtracting this from each frame. The calcium green signals (i.e. 475 nm measurements) were calculated as $\Delta F/F$, where the mean of all frames measured was used as F. These measurements were corrected for bleaching by fitting a logarithmic function. In the case of fura-recordings, we calculated the ratio 340 nm / 380 nm and multiplied it with 100. Since each glomerulus had an individual background fluorescence, all time traces were shifted to zero shortly before the stimulus onset by subtracting the background using frames 5-9 (i.e. before stimulus); these values are labeled as Δ(F340/F380) [%] in the figures. This allows a comparison between the traces of different glomeruli. For false-color display (Figs. 1, 2A) at each pixel a square of 11 x 11 pixels was

averaged in its time course; the mean value between frames 12-24 (i.e. from stimulus onset until 1 s after stimulus offset) is shown for each pixel.

We reconstructed the glomerular borderlines in the fura ratio images (Fig. 1B) and mapped the calcium signals to identified glomeruli using the digital atlas of the honeybee AL (Galizia et al. 1999a). This method has already been used in our previous studies (Galizia et al. 1999b; Sachse et al. 1999; Sachse and Galizia 2002). To calculate the numbers of activated and inhibited glomeruli (Figs. 2B, 5C) we counted all glomerular calcium increases and decreases greater than noise limit, respectively. Noise was estimated for each animal as the standard deviation of the response between frames 4-11 averaged over all measurements in one animal. All values within the noise limit were clipped to zero. For the signals' amplitude (Fig. 2D) we computed the maximum during frames 12-24 (i.e. from onset until 1 s after stimulus offset); the signals' duration (Fig. 2E) was calculated at their half-maximal response. Both the calcium signals' amplitude as well as its duration were odor concentration-dependent (Figs. 2C, D, E). In order to include both parameters, we used the integral of the glomerular response to calculate the glomerular activation in each animal (Figs. 3, 4, 6). The calcium green signals (compound responses) revealed a higher latency than the fura signals (PN responses). We used the integral covering frames 12 to 30 for the compound responses and frames 12 to 24 for the PNs (i. e. from stimulus onset until 2s or 1s after stimulus offset) as the glomerular activation to include comparable parts of the calcium signals for both dyes. Within each animal we took the mean response of 2 measurements for each odor and concentration. We calculated the glomerular inhibition by measuring the minimum during stimulus application.

In order to average the glomerular responses over all measured animals, the animal's glomerular activations were normalized in two different ways according to the respective approach. We set the strongest glomerular response in each animal to this particular odor at 1 and scaled the other responses accordingly (Fig. 3) to allow a comparison of the dose response functions between different glomeruli stimulated by the same odor. A comparison of these normalized response intensities between dose response functions to different odors is not meaningful, since they are scaled to different values. Therefore in a parallel analysis, we set the strongest glomerular activation across all measured odors and glomeruli in each animal at 1 and scaled all other responses relative to it (Fig. 4A, B). This allows comparing the dose response function to different odors within one glomerulus. For example, the compound response of glomerulus 28 to hexanol showed the maximal activation for the highest concentration (Fig. 4A), whereas the PN response was strongest in glomerulus 33 to nonanol (Fig. 4B). We fitted each dose response function to the Hill equation using a least-square optimization (see RESULTS). From this function we calculated the half-saturating concentration (Ki), the sensitivity (1/Ki) and the Hill coefficient as a measure of the slope (n) for a subset of identified glomeruli to each tested odor (Tab. 1).

Each odor representation can be regarded as a vector in a multidimensional space, where each glomerulus represents one dimension. We used principal component analyses (PCA) to visualize the relative odor representations in a reference system with reduced dimensionality (Fig. 6B). This technique calculates a new cartesian coordinate system based on the eigenvectors of the correlation matrix in which the first axis (i.e. the first principal component) explains most of the variance observed, the second most of the remaining variance, etc. We included a varimax rotation of the first two principal components to make the factors more interpretable. The PCA were performed using SPSS (SPSS Inc., Chicago, IL).

RESULTS

Simultaneous measurements of different AL neuron populations

Using two different calcium-sensitive dyes in one animal it is possible to visualize the calcium response properties of different neuron populations and thus to simultaneously measure different processing levels in the AL. In this case distinct calcium responses should be measurable for each dye. We used a bath-application of the membrane-permeable calcium green-AM to stain all neurons in the AL (RNs, LNs and PNs) and measured a 'compound signal' as a calcium response, which is dominated by the input to the AL (Fig. 1A; see DISCUSSION). Without any stimulation the glomeruli revealed no calcium changes above noise level, whereas an odor application of 1 s led to a strong, reliable and long-lasting calcium increase in several glomeruli. The time courses showed an exponential decrease during the measurements due to the bleaching of the calcium green dye, which was corrected by subtracting a logarithmic curve fitting the bleaching decrease (see METHODS). Since this correction could not completely eliminate the bleaching, this artifact is still visible in the time courses of the compound measurements.

With the second and membrane-impermeable calcium-sensitive dye, fura-dextran, we selectively backfilled and measured the PNs of the lateral ACT, which represent the output of the superficial glomeruli (Fig. 1B). This method was already established and has been used previously (Sachse and Galizia 2002). A successful loading of the PNs was apparent, when the somata of the lateral ACT neurons were stained (arrows in Fig. 1B) and when the glomerular structure was visible in the fluorescence ratio image. Thus, we could reconstruct the glomerular borderlines and map the calcium signals to morphologically identified glomeruli, which allows a comparison between different individuals.

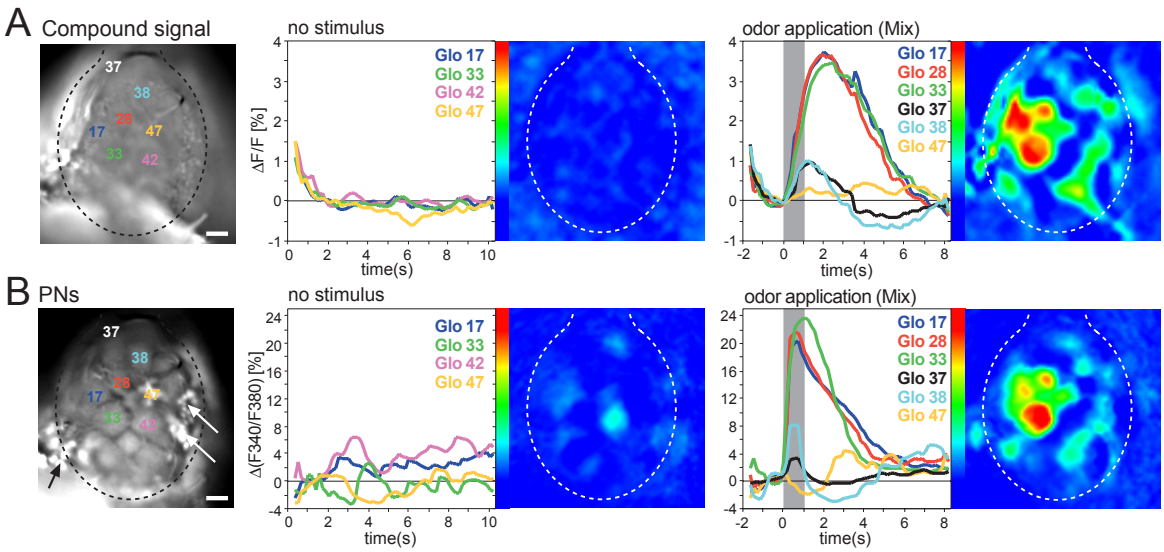

Figure 1 Simultaneous measurements of two calcium-sensitive dyes in one animal.
A, *Left*, morphological view of the AL when all AL cells were stained with a bath-application of the membrane-permeable dye calcium green-2 AM. The AL border is marked with a dotted line, antennal nerve is at the top. A subset of glomeruli has been identified using the digital AL atlas. *Middle*, *right*, time traces of calcium-green responses in identified glomeruli and false-color-coded spatial response patterns during measurement without and with odor application. Odor used was a tertiary mixture of the three alcohols hexanol, octanol and nonanol. **B**, *Left*, morphological view of the AL of the same animal as in A, in which the l-ACT neurons have been selectively stained with the calcium-sensitive dye fura-dextran. The glomerular structure is visible, which allows identification of the glomeruli. *Middle*, *right*, time traces of fura responses in identified glomeruli and false-color-coded activity patterns without and with odor stimulation of the identical measurement as shown in A. In contrast to the compound signal the PNs are spontaneously active. For both staining methods odor application leads to a strong calcium increase. Note that PNs can also be inhibited during olfactory stimulation (e.g. glomerulus 47). Scale bar, 50 µm.

In contrast to the compound signals PNs revealed a high amount of spontaneous activity in the absence of any odor (compare Fig. 1A and B). Odor stimulation evoked both excitatory (e.g. glomerulus 17, 28 and 33 in Fig. 1B) as well as inhibitory responses (e.g. glomerulus 47 in Fig. 1B) in PNs. Furthermore, the PN responses had a briefer latency and did not last as long as the compound signals. Neither spontaneous activity nor inhibitory responses were seen in the compound signals, confirming that it is possible to measure both dyes independently from each other (see DISCUSSION). Excitation relationships between the activated glomeruli were not equal for the compound signals and the PNs. In the example shown in Figure 1, glomeruli 17, 28 and 33 were activated similarly in the compound signal, whereas the PN response was stronger for glomerulus 33 than for glomeruli 17 and 28.

Spatial and temporal activity patterns are concentration-dependent

We measured spatio-temporal dose-response curves to the three odors 1-hexanol, 1-octanol and 1-nonanol diluted in 7 log units in the solvent mineral oil. Increasing odor concentration led to an increased number of activated glomeruli. For example, the odor hexanol (Fig. 2A) elicited the first detectable signals in glomerulus 17 (white arrow in Fig. 2A).

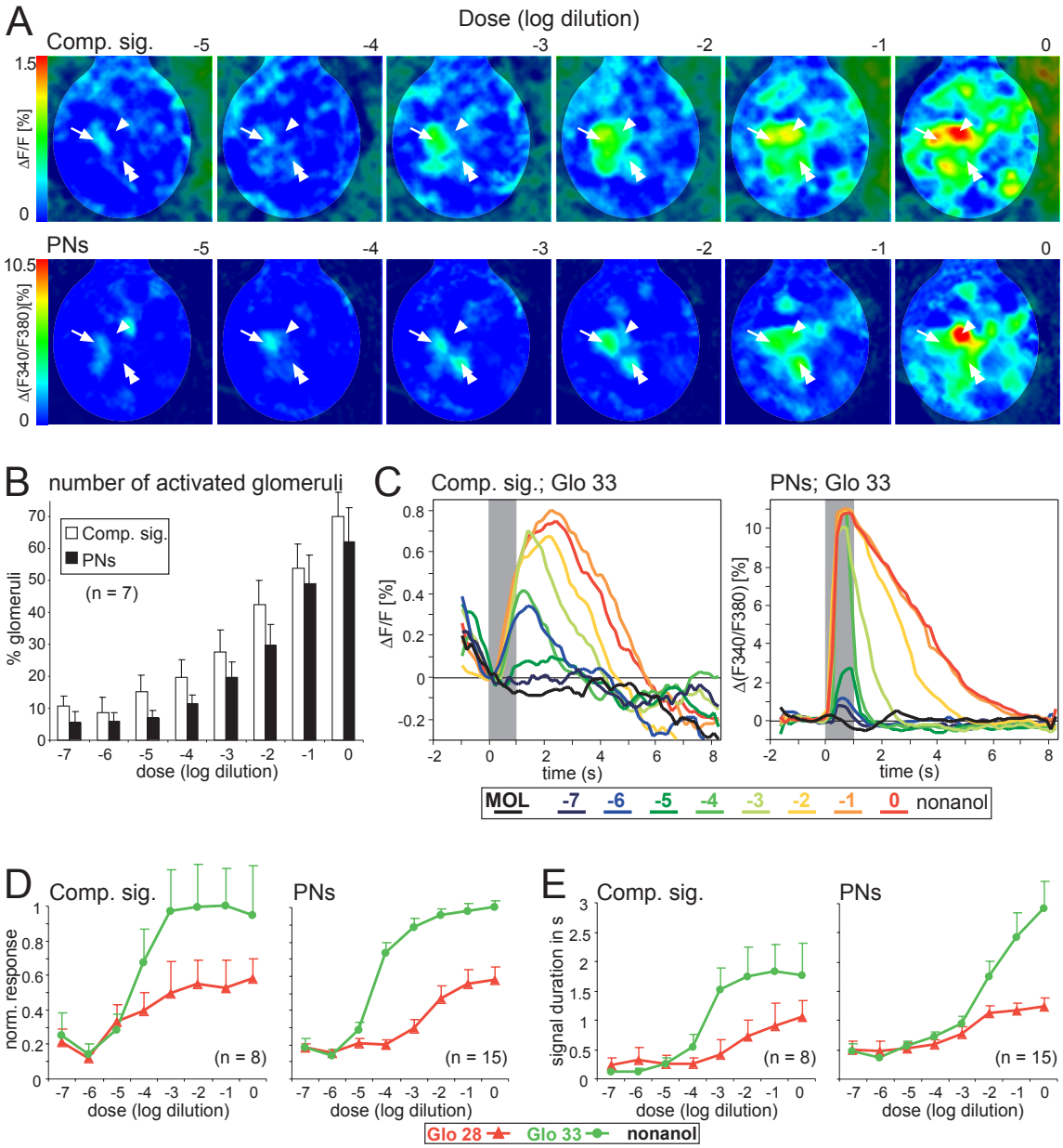

Figure 2 Increasing odor concentration leads to a recruitment of more glomeruli.
A, False-color coded spatial activity patterns of the compound signals (above) as well as the PN responses (bottom) to hexanol stimulation over a concentration range of 5 log units. The area outside the AL has been shaded. For comparison the positions of glomeruli 17 (arrow), 28 (arrowhead) and 33 (double arrow) are marked in each image. It is apparent that increasing concentration activates increasing numbers of glomeruli. Note that glomerulus 17 reveals the first detectable signals at low concentration, whereas glomerulus 28 dominates the pattern at the highest concentration. **B**, Percent of activated glomeruli of the compound signal (white bars) as well as the PN response (black bars) averaged over all odors and identical animals for both staining procedures; error bars (SEM) and n relate to animals. Both show a significant increase of active glomeruli with increasing odor concentration. Note that the compound signals comprise a higher number of activated glomeruli than the PNs at each concentration level. **C**, Time traces of glomerulus 33 to nonanol stimulation. Stimulus is given by the gray shading. The odor concentration is coded by the different colors. For both the compound signal as well as the PN response increasing nonanol concentration leads to an increase in the signal amplitude and duration until saturation.

D, **E**, Plots of signal amplitudes (D) and duration (E) versus concentration for glomeruli 28 and 33 to nonanol concentration averaged over all individuals. Error bars indicate means and SE values. Strongly- as well as intermediately-activated glomeruli show an approximately sigmoidal curve. Note that the number of bees differ between staining procedures (see METHODS).

With increasing odor concentration glomeruli 33 (double arrowhead) and 28 (arrowhead) also became activated. The latter was finally the dominant glomerulus for the highest odor concentration. The AL network led to a change in the relative responses. For example, glomerulus 28 dominated the PN response at the highest concentration, whereas glomerulus 17 revealed the same excitation level as glomerulus 28 for the compound signal. The concentration-dependent recruitment of activated glomeruli was seen in all preparations for all odors tested (Fig. 2B), resulting in activity patterns that differ for different odor concentrations. These findings are consistent with several optical recording studies of the olfactory bulb of rats, mice and zebrafish (Friedrich and Korsching 1997; Rubin and Katz 1999; Johnson and Leon 2000; Fuss and Korsching 2001; Meister and Bonhoeffer 2001; Wachowiak and Cohen 2001) as well as studies of the honeybee and moth AL (Sachse et al. 1999; Galizia et al. 2000). Interestingly, the compound signals comprised a higher number of activated glomeruli (70% of the imaged glomeruli for the highest concentration; Fig. 2B) than the PN activity patterns (62% of the imaged glomeruli).

The responses increased in amplitude and duration with increasing odor concentration until a saturated maximum. An example for the time courses of an identified glomerulus during stimulation with nonanol at increasing concentrations (marked by the different colors) is shown in Figure 2C. The compound signal and the PN responses showed a similar concentration dependence; both revealed a successive increase and prolongation of the calcium response following the increasing concentration. The maximal amplitude and signal duration of two identified glomeruli during nonanol stimulation averaged over all animals is represented in Figure 2D and E. Both parameters reveal a saturation level at a specific concentration even for only intermediately-activated glomeruli (glomerulus 28, red line). However, the compound signals seem to saturate in signal amplitude and duration at a lower concentration level compared to the PN responses. In contrast to other studies (Firestein et al. 1993; Duchamp-Viret et al. 1999; Duchamp-Viret et al. 2000; Spors and Grinvald 2002) the latency of the odor responses did not significantly change with increasing odor concentration. Since concentration-dependent changes in latency were reported to be in the range of 80 ms (Spors and Grinvald 2002), our temporal resolution of 6 Hz might be too low to observe these effects. On average, the compound signals reached their half-maximum value 1200 ms after stimulus onset, whereas the PN responses took only 200 ms (data not shown). These different latencies appear to contradict their cellular sources, since one would expect to observe the input signals shortly before or at least synchronously with the output signals of the AL. However, this synaptic delay is in the range of only a few milliseconds and there-

fore below our temporal resolution. The observed difference in calcium-response dynamics must therefore reflect differences in the calcium influx and buffering mechanisms of the measured cells. Other calcium imaging studies, where the afferents were selectively labeled with calcium green dextran, showed almost identical latencies as our calcium green signals (Friedrich and Korsching 1997; Wachowiak and Cohen 2001; Wachowiak et al. 2002). Moreover, electrophysiological recordings in frogs showed that late and sustained RN activities did not coincide with early peaks of bulb neurons involved in intensity coding, suggesting that convergence, in association with intraglomerular processing, is involved in changing the temporal structure of the olfactory information (Duchamp-Viret et al. 1990a).

Dose-response functions of the input and the output neurons

Since both the signal amplitude as well as the signal duration are concentration-dependent (Fig. 2D and E), we defined the integral covering frames 12 to 24 for the PNs and frames 12 to 30 for the compound responses (i. e. from stimulus onset until 1s or 2s after stimulus offset) as the glomerular activation. We calculated the dose response functions for the tested odors by averaging all measured animals. In total the dose response curves were measured for 32 glomeruli, of which 6 glomeruli are shown in Fig. 3, tested with 8 concentrations over a range of 7 log units. Each odor-evoked specific dose response functions in identified glomeruli. Most of the dose response curves are sigmoidal, with their rising phase spanning up to 4 log units. Note that the curves are normalized to the maximum glomerular response within each odor. Thus, a comparison of the response intensities of specific glomeruli between the different odors is not possible in this figure. In the compound signals, hexanol elicited the first responses in glomerulus 17 (blue curve) at a concentration of 10^{-4}. Since glomerulus 28 revealed a steeper slope (red curve), its response ended above that of glomerulus 17 at the highest concentration. The dose response functions of the other glomeruli were shifted to higher concentrations. For hexanol the glomerular responses did not saturate, possibly because of insufficient receptor activation. Octanol was clearly dominated by glomerulus 17, which was already activated above noise threshold at a concentration of 10^{-6}. Responses to nonanol were also first detectable in glomerulus 17. However, at a concentration of 10^{-2} glomerulus 33 (green curve) took over and dominated the activity pattern. The dose response functions of the PNs showed similar properties (Fig. 3Aii); most of the curves were sigmoidal with a dynamic range also spanning up to 4 log units as for the compound curves. In order to simplify a comparison between the compound signal and the PNs we replicated the dose response functions shown in Figure 3A, and superimposed them for three glomeruli each, in Figure 3Bi and Bii. The dose response functions of the most sensitive glomeruli (e.g. glomerulus 28 for hexanol, glomerulus 17 for octanol and glomerulus 33 for nonanol) are almost identical for both neuron populations.

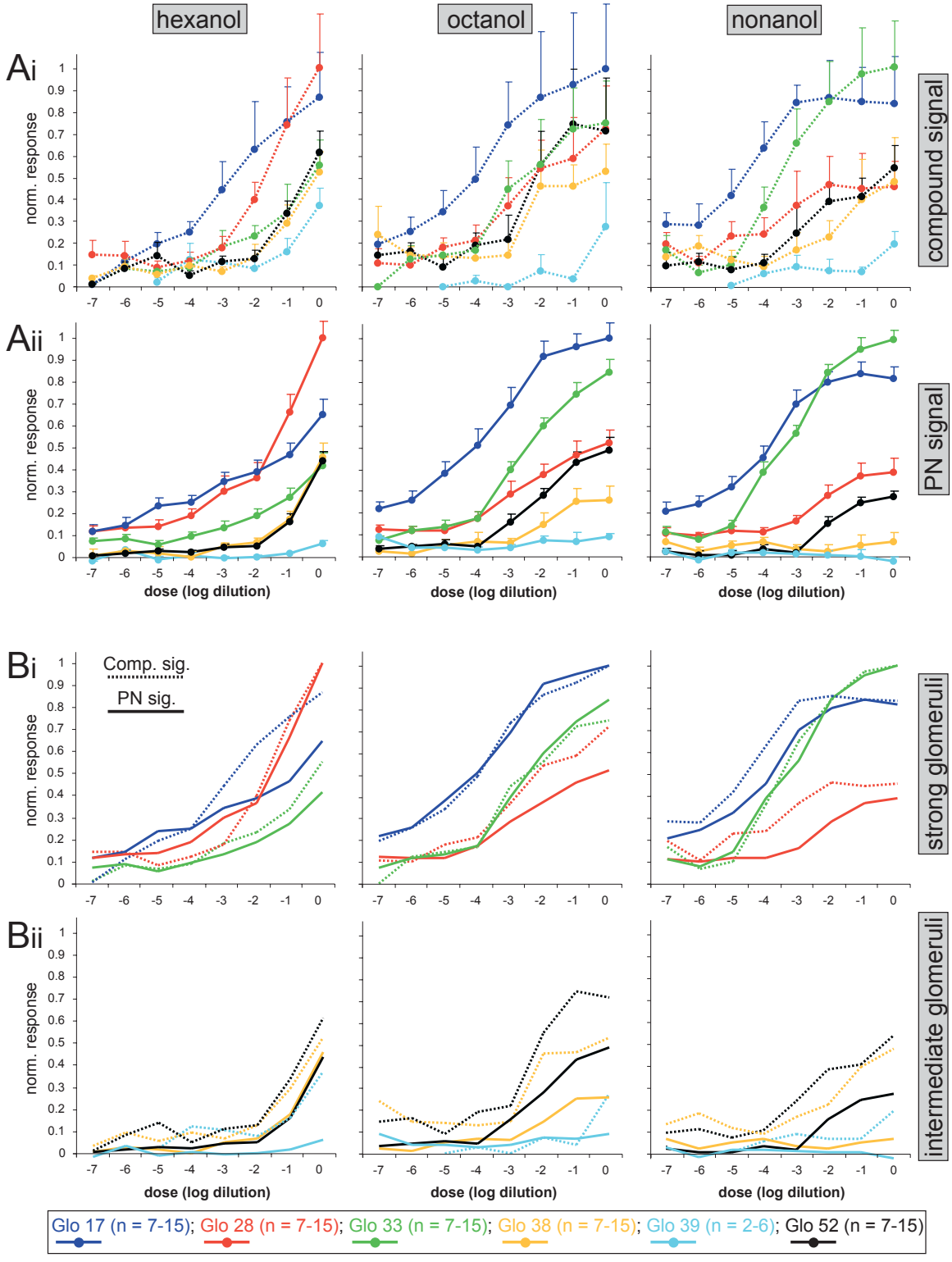

Figure 3 Dose-response functions of different identified glomeruli to a specific odor.
A, Compound responses (dotted lines, Ai) and PN responses (solid lines, Aii) of 6 identified glomeruli to the three primary alcohols hexanol, octanol and nonanol to 8 concentrations averaged over all animals measured (means and SEM). The responses have been normalized by setting the strongest glomerular response in each animal for each odor at 1 and scaling the other responses accordingly to eliminate individual differences in response intensity. Thus, a comparison between the dose-response functions of

different odors is not meaningful. Most of the dose-response curves are sigmoidal, whereas some curves do not saturate. **B**, For comparison between the compound and the PN dose-response functions, the same curves as in A were superimposed, separated in strongly- (Bi) and intermediately- or weakly-activated glomeruli (Bii). In all cases the dose-response curves of the compound signal are either identical or above the curves of PNs, indicating that the signals on the PN level are more confined compared to the compound signal.

However, the intermediately-activated glomeruli reveal strong differences between the compound signals and the PNs. For example, the dose response functions of glomerulus 17 for hexanol, glomerulus 28 for octanol and glomeruli 17 and 28 for nonanol were all shifted to a higher concentration and thus were less sensitive in the PN response. The weakly-activated glomeruli even showed no PN response, although they were activated in the compound pattern (glomeruli 38 and 39).

In Fig. 4A and B these curves were normalized to the maximum glomerular response including all odors. Glomerulus 28 was most sensitive to hexanol, whereas octanol and nonanol elicited similarly weak responses. Glomeruli 17 and 33 showed their strongest responses to nonanol, intermediate and weak responses to octanol and hexanol, respectively. The last two glomeruli are examples for glomeruli whose response strength is dependent on the carbon chain length of the odor molecule (Rubin and Katz 1999; Sachse et al. 1999; Uchida et al. 2000; Meister and Bonhoeffer 2001). Again, comparison of the dose response curves of both neuron populations reveals that some are right-shifted in their output. We quantified these observations by fitting the dose response functions to the Hill equation (1):

$$R = R_{max}\frac{C^n}{C^n + K_i^n}$$

In this equation, R is the measured response amplitude, R_{max} is the maximal response, C is the odor concentration, n (Hill coefficient) is a measure of the slope and K_i is the half-saturating concentration. For a given glomerulus the response strength to a specific odor is determined by its parameter K_i. We therefore defined the sensitivity of a particular glomerulus to a specific odor as the inverse of K_i (definition after Meister and Bonhoeffer 2001). The sensitivity of the three prominent glomeruli for the compound signals and the PNs to the tested odors is graphically shown in Figure 4C.

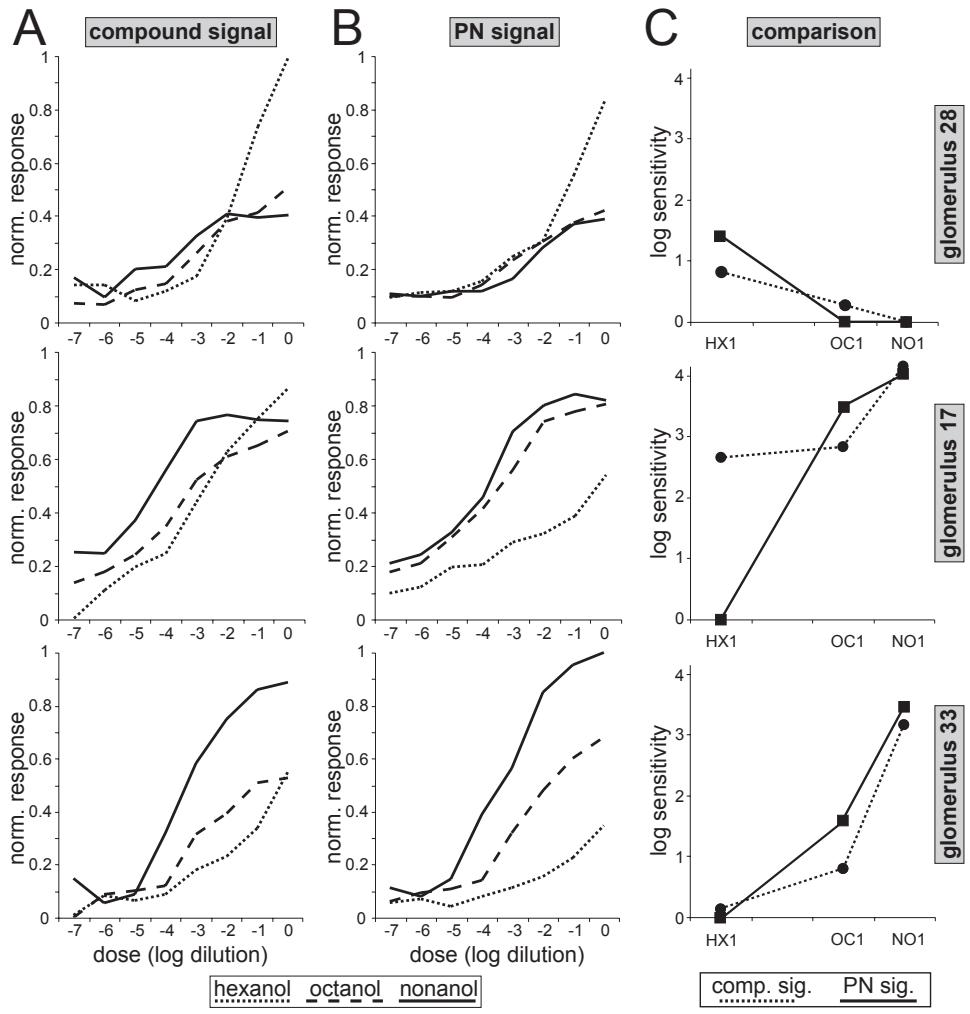

Figure 4 Dose-response functions and sensitivities of identified glomeruli to different odors. **A**, **B**, For each of the three identified glomeruli 28, 17 and 33 their dose response curves to all three alcohols are represented in one plot for the compound signal (A) as well as for the PN response (B). The curves are normalized to the strongest glomerular response in all three odors. Hexanol elicited the strongest response in glomerulus 28, whereas glomeruli 17 and 33 are activated the strongest by nonanol. Note that each odor elicits at least an intermediate compound response in each glomerulus, whereas some of these responses are reduced and thus confined on the PN level. Same data as in Fig. 3, but with different normalization. **C**, Sensitivities (defined as the inverse of the half-saturating concentration Ki) of the same three glomeruli as in A and B to the three tested alcohols hexanol (HX1), octanol (OC1) and nonanol (NO1) of the compound and PN signals. The data are represented logarithmically. The arrangement of the three odors reflects their chemical similarity. The sensitivity differs in an odor-specific manner for the compound and PN responses.

Table 1 summarizes all parameters, as the K_i-values, the sensitivities and the Hill coefficients of a subset of glomeruli during measurements of the compound signals (C; dark gray) and the PN responses (PN; bright gray), respectively. Consideration of the strongly-activated and prominent glomeruli for each of the three odors (glomerulus 28 for hexanol, 17 for octanol and 33 for octanol and nonanol) shows that these have much lower K_i-values

and thus a higher sensitivity on the PN level than for the compound response (Fig. 4C, Tab.1).

Glo	Odor	Ki-value	sensitivity	Hill coeff.	sig.	n
17	HX1	$2.2 * 10^{-3}$	454.55	0.30	C.	7
		$9.4 * 10^{-1}$	1.06	0.14	PN	13
	OC1	$1.5 * 10^{-3}$	666.67	0.25	C.	7
		$3.2 * 10^{-4}$	3125.0	0.22	PN	14
	NO1	$7.0 * 10^{-5}$	14285.7	0.24	C.	8
		$9.7 * 10^{-5}$	10309.3	0.24	PN	15
28	HX1	$1.5 * 10^{-1}$	6.67	0.56	C.	7
		$3.8 * 10^{-2}$	26.32	0.31	PN	13
	OC1	$5.3 * 10^{-1}$	1.89	0.18	C.	7
		$(5.2 * 10^{0})$	(0.19)	(0.15)	PN	14
	NO1	$(6.0 * 10^{0})$	(0.17)	(0.10)	C.	8
		$(1.4 * 10^{1})$	(0.07)	(0.14)	PN	15
33	HX1	$7.4 * 10^{-1}$	1.35	0.25	C.	7
		$(4.9 * 10^{1})$	(0.02)	(0.19)	PN	13
	OC1	$1.6 * 10^{-1}$	6.25	0.21	C.	7
		$2.5 * 10^{-2}$	40.0	0.25	PN	14
	NO1	$6.8 * 10^{-4}$	1470.59	0.39	C.	8
		$3.5 * 10^{-4}$	2857.14	0.45	PN	15
38	HX1	$1.0 * 10^{0}$	1.0	0.35	C.	7
		$(2.6 * 10^{0})$	(0.38)	(0.51)	PN	13
	OC1	$(4.6 * 10^{0})$	(0.22)	(0.20)	C.	7
		$(7.1 * 10^{2})$	(0.001)	(0.18)	PN	14
	NO1	$(1.5 * 10^{1})$	(0.07)	(0.15)	C.	8
		—	—	—	PN	15
52	HX1	$4.5 * 10^{-1}$	2.22	0.40	C.	7
		$(3.0 * 10^{0})$	(0.34)	(0.53)	PN	12
	OC1	$2.8 * 10^{-1}$	3.57	0.21	C.	7
		$(3.7 * 10^{0})$	(0.27)	(0.23)	PN	13
	NO1	$(1.4 * 10^{0})$	(0.71)	(0.18)	C.	8
		$(2.8 * 10^{1})$	(0.04)	(0.24)	PN	14

Table 1: Strongly-activated glomeruli display an increased sensitivity on the PN level compared to the compound responses, whereas the sensitivity of lower-activated glomeruli is reduced.
Summary of K_i-values, sensitivities (i.e. $1/K_i$) and Hill coefficients obtained for the five mostly highly-activated glomeruli tested with all three odors over a concentration range of 7 log units. These parameters are listed for the compound (C., dark gray) and the PN response (PN, bright gray); numbers of animals are given in the last column (n). Parameters were calculated by fitting the dose-response functions to the Hill equation (1). The dose-response functions were normalized as described in Figure 4A, B. The values of dose-response functions which did not achieve their half-saturating concentration were estimated and are therefore shown in brackets. Empty entries indicate responses below noise limits, i.e. no dose-response function could be fitted.

In contrast, weaker glomeruli showed higher K_i-values and lower sensitivities on the PN level as compared to the compound signals. The fitted slopes revealed various Hill-coefficients from 0.14 to 0.56, indicating that different glomeruli can have different dose-response functions. Remarkably, the strongly-activated glomeruli have higher Hill-coefficients (i.e. steeper slopes) than the weaker-activated glomeruli. For example, the PN dose-response function of glomerulus 33 had a Hill-coefficient of 0.45 to nonanol, whereas glomeruli 17 and 28 had values of only 0.24 and 0.14, respectively (Tab. 1). The slope and thus the dynamic range of an identified glomerulus to a specific odor was quite similar for the compound response and its output. This is different from vertebrates, where electrophysio-

logical recordings showed a difference in the intensity tuning range for RNs compared to bulb neurons: Single-cell-recordings of individual RNs have a dynamic range typically spanning only 1-2 log units of concentration (Firestein et al. 1993; Trotier 1994; Duchamp-Viret et al. 2000) and thus have Hill coefficients from 1.9 to 4.4 (Firestein et al. 1993), as opposed to a range of 2-4 log units in mitral cells (Duchamp-Viret et al. 1990a). Since the latter value matches our measured dynamic range of PNs, the discrepancy lies in the RN data. Indeed, electrophysiological recordings of honeybee RNs showed narrow tuning ranges, as found in vertebrates (Vareschi 1971). The larger dynamic range measured in this study is therefore probably due to the fact that we measured averaged signals of all RNs converging onto single glomeruli. In consequence, individual receptor capacities with their narrow intensity tuning curves add up to an overall response with a much broader dynamic range (Cleland and Linster 1999), which is in accordance with other optical recording studies (Friedrich and Korsching 1997; Fuss and Korsching 2001; Wachowiak and Cohen 2001; Wachowiak et al. 2002).

Effects of odor concentration on inhibited glomeruli

In the PN signals odors evoke both excitation and inhibition (Sachse and Galizia 2002). Inhibitory responses are caused by inhibitory local interneurons and are therefore only visible in the output responses, not in the compound signals. These inhibitory PN responses were also dependent on the odor concentration. For example, the odor-evoked calcium decrease of glomerulus 56 increased in negative amplitude and duration with increasing concentration of nonanol (Fig. 5A). We calculated the dose-response functions of inhibited glomeruli averaged over all measured animals; three of them are represented in Fig. 5B. All three glomeruli showed an increased inhibitory response with increasing odor concentration. Inhibition of glomeruli 25 and 29 saturated for the highest concentration. The maximum number of inhibited glomeruli appeared at odor concentrations of 10^{-5} and 10^{-4}, and decreased with increasing concentration (Fig. 5C). More olfactory receptor types become activated with increasing odor concentration (Vareschi 1971; Firestein et al. 1993; Duchamp-Viret et al. 2000), which is also apparent in the responses of unspecific glomeruli in the compound signal at high concentrations (Fig. 3). Therefore this increase is likely to counterbalance the cross-glomerular inhibitory connections, and thus reduces the number of inhibited glomeruli on the output level of the AL.

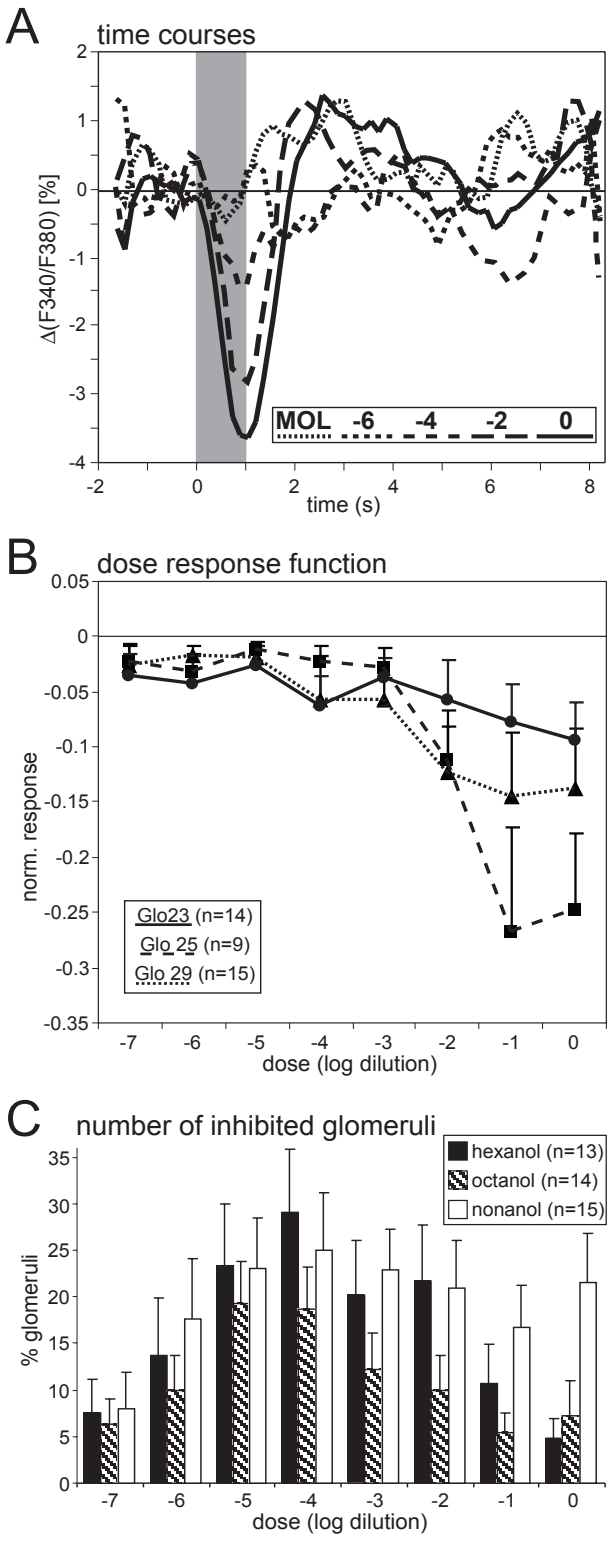

Figure 5 In contrast to the compound signals, PNs showed inhibitory responses, which are also concentration-dependent. **A**, Time traces of glomerulus 56 to nonanol stimulation. Stimulus is shown by the gray shading. The odor concentration is coded by the different line styles. As for the excitatory responses, increasing nonanol concentration increases the signal amplitude and duration. **B**, Dose-response functions of three identified glomeruli to 8 concentrations of nonanol averaged over all individuals (means and SEM). The responses have been normalized by setting the strongest inhibitory response in each animal for each odor at 1 and scaling the other responses accordingly. **C**, Percent of inhibited glomeruli to all three odors averaged over all animals measured. The number of inhibited glomeruli is maximal for intermediate concentrations.

Increasing odor concentration increases odor discriminability

We analyzed whether the odor similarities are concentration-dependent or if the odor-evoked activity patterns retain their odor-specificity. We therefore represented the odor patterns in a three-dimensional space based on the response intensities of the three strongest

and prominent glomeruli for the tested odors (glomeruli 17, 28 and 33 for octanol, hexanol and nonanol, respectively). Arranging the data in this way reveals that the compound responses (Fig. 6Ai) above a concentration of 10^{-3} and the PN responses (Fig. 6Aii) above 10^{-4} are clearly separable and are ranked from the center to the periphery of the space with increasing concentration, whereas the activity patterns to lower concentrations are clustered in the center. This clustering reflects the weaker overall activity elicited by low concentrations. We therefore calculated the excitation ratio as a vector between these three glomeruli for each odor at each concentration. Comparison of the compound activity patterns with the PN patterns shows that the three odors hexanol, octanol and nonanol are represented separately in three clusters on the PN level with exception of the very low concentrations, whereas the compound patterns are almost clustered together. One reason for this difference is the strong contribution of glomerulus 17 to hexanol in the compound response, but not in the PN response (Fig. 3Bi, 4A, B). We next analyzed whether discrimination improves when all frequently-imaged glomeruli (n=23) are taken into account, again taking each glomerulus as an independent dimension in a multidimensional space. Using a principal component analysis (PCA; see METHODS) it is possible to visualize the relative positions of the odor responses in a reference system with reduced dimensionality. The PCA reveals that most of the variance could be represented in a two-dimensional space, therefore only the first and second principal components are shown (Fig. 6B). Including all glomeruli separates the odor representations to a lesser extent than would be the case if using only the three strongest glomeruli. The compound signals of hexanol were separated from octanol and nonanol only at the highest two concentrations. The activity patterns of octanol at higher concentrations appeared differentiated from nonanol for the third principal component (not shown). When excluding the three most sensitive and thus prominent glomeruli (i.e. glomeruli 17, 28 and 33), the arrangement of the odor responses appeared almost identical, indicating that weakly-activated glomeruli contain considerable information about the olfactory stimulus. Interestingly, the multidimensional representations reflected the chemical similarity of the odors. Activity patterns evoked by octanol were arranged in between those of hexanol and nonanol, but closer to the latter. The ‘gap’ between hexanol and octanol would probably be filled by glomerular responses to heptanol.

Accordant to electrophysiological recordings of frog RNs (Duchamp-Viret et al. 1990b), these analyses show that the probability of discrimination increases with stimulus intensity, since the further the odor is located from the center, the longer its distance from the other odors. The continuity of RN recruitment, which leads to the PNs becoming more and more active with increasing stimulus concentration, probably coincides with a more detailed description of the odors.

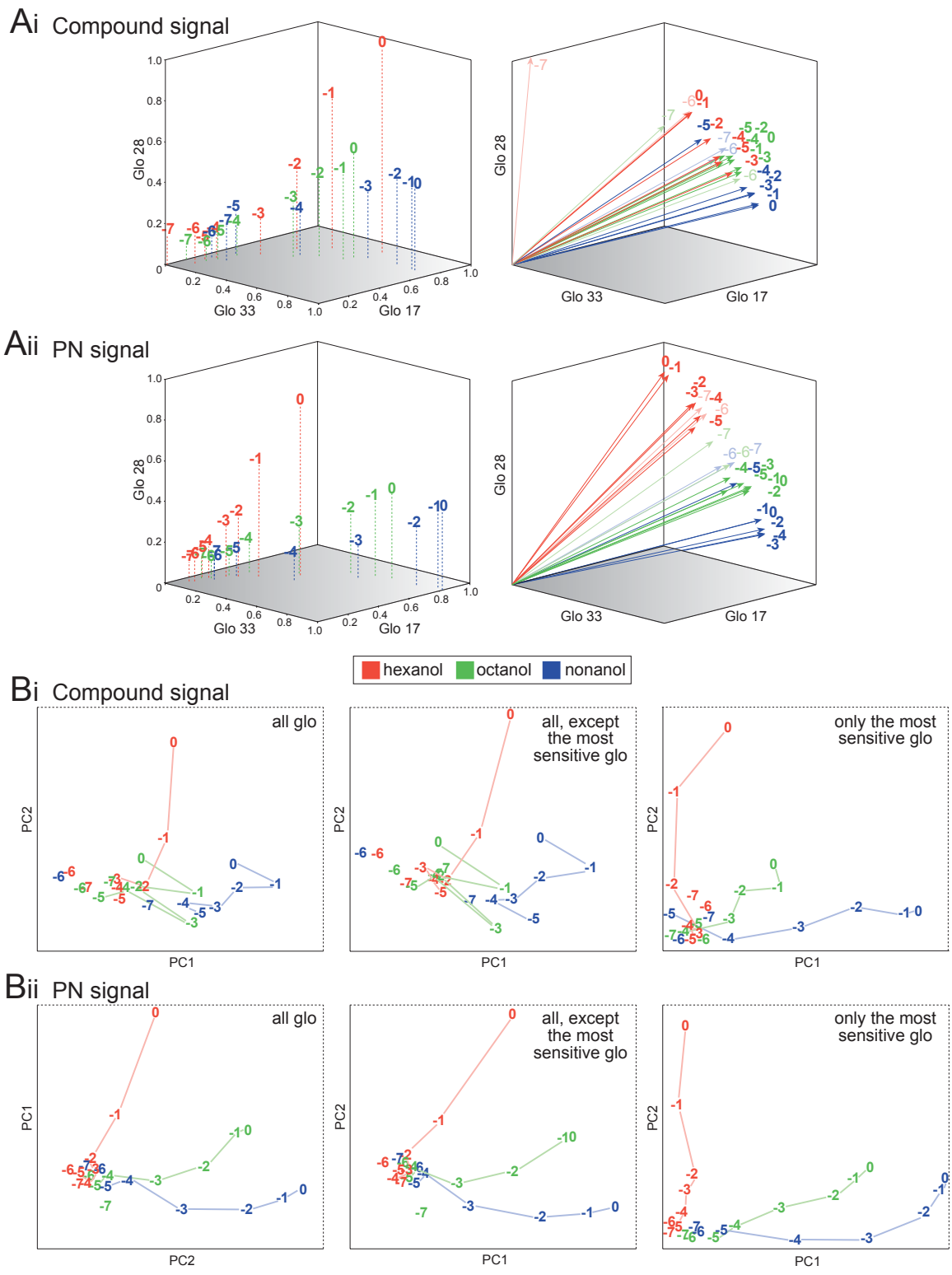

Figure 6 Increasing odor concentration leads to activity patterns becoming less similar to each other.

A, The averaged compound (Ai) as well as PN activity patterns (Aii) to the three alcohols over 8 concentrations are represented in a 3-dimensional space defined by the normalized response intensity of the three strongest glomeruli (left; as shown in Fig. 4A, B) and their relative excitation ratios (right). Each activity pattern can be represented as a point in space or a vector with a specific length (response intensity)

and direction (relative excitation). Transforming these vectors to unit length corrects for unequal response intensities (right). The colors indicate the odor, the numbers the odor concentration. Both representations reveal that the three odors are more clearly separated at the PN level than as compound patterns. **B**, Principal component analyses (PCA) of the compound (Bi) and PN responses (Bii), performed on all measured individuals for all three odors. In the analyses we included either all 23 most frequently recognized glomeruli (left), all except the three most sensitive glomeruli (i.e. 17, 28 and 33, middle) or only these most sensitive glomeruli (corresponding to the data in A, right). The projection in the two-dimensional plane accounts for most of the variance (comp. sig.: 76%, 82% and 97%; PN: 88%, 88% and 98%, respectively). The best separation of the stimuli is obtained when only the three most sensitive glomeruli are considered in the analysis. In all cases the separation of odor-specific responses improved with increasing concentration.

DISCUSSION

In this study, we used calcium imaging in the honeybee to investigate the processing of odor quality and intensity by the AL network. To this end, we simultaneously measured input and output to the AL when stimulating with different odors at varying concentrations. We combined a protocol which emphasizes the RNs with a PN-selective protocol. A comparison of the two provides evidence that the primary olfactory signals are modulated and contrast-enhanced by the AL network to improve both concentration-invariance for odor quality detection and the sensitivity of the olfactory system.

Methodological considerations

Fura-dextran was locally applied to the lateral ACT in order to selectively stain uniglomerular PNs, which innervate the superficial glomeruli, whereas the calcium green-2AM was bath-applied to the whole AL to measure the RNs. Since the AM ester allows the dye to permeate cell membranes, all cells in the AL (RNs, LNs, PNs and glia cells) could be stained. However, we propose that the major contribution to the calcium signals comes from RNs for two reasons: first, the RNs numerically dominate in the AL (see INTRODUCTION), and second, inhibitory responses, which have been shown for LNs and PNs, have never been seen (Joerges et al. 1997; Galizia et al. 1998; Galizia et al. 1999b; Sachse et al. 1999). Thus, we take the compound signals as a measure of the functional innervation pattern to the olfactory glomeruli in the AL (i.e. the input), only moderately modified by lateral connections of the LNs.

Calcium signals deriving from the two dyes could be measured separately. In control experiments when we applied only one staining protocol at a time, we observed no or only weak signals at the wavelength for the other, non-used dye (data not shown). This is further confirmed by the different response properties of the two neuron populations. In contrast to the compound responses, the PN signals showed spontaneous activity in the absence of a stimulus (Fig. 1), a shorter latency and lasted only until the stimulus offset for intermediate

odor concentrations. This difference meets our expectations as PN signals underwent intraglomerular processing by the AL network. Furthermore, the compound differed from the PN responses in signals that could be observed in glomeruli which showed no calcium response in their PNs (e.g. glomeruli 38 and 39 to nonanol in Fig. 3), and in the time-course of the response (Fig. 1, Fig. 2C).

The output odor representation is optimized compared to the input

With increasing odor concentration the receptive range of individual RNs becomes broader (Vareschi 1971; Akers and Getz 1993; Firestein et al. 1993; Duchamp-Viret et al. 2000; Ma and Shepherd 2000; de Bruyne et al. 2001) leading to a decrease of their odor-specificity. This broadening has to be corrected by the olfactory system to ensure reliable odor discrimination. Indeed, our results show that the AL network improves the afferent input by sharpening the glomerular response profiles and thus contrast-enhances the representations of different odors. The dose-response functions of weakly- or intermediately-activated and thus 'secondary' glomeruli were shifted towards higher concentrations, which led to a lower number of glomeruli showing an excitatory output compared to the input signal (Figs. 2B, 3, Tab. 1). Contrary, the relative responses of the most responsive and thus 'primary' glomeruli changed in an odor-specific manner. The sensitivity of glomeruli which were the strongest at the highest odor concentration was increased on the output level (e.g. glomerulus 28 for hexanol and 17 for octanol; Tab. 1), while the relative responses of a few others which dominated the activity patterns at low concentrations were reduced (e.g. glomerulus 17 for hexanol or nonanol). As a result, each odor elicited activity in only a few glomeruli even at very low concentrations. Our findings are in line with a comparative electrophysiological study of frog RNs and second-order neuron sensitivities, which reported that the response thresholds within second-order neurons to specific odors were significantly lower than thresholds in RNs (Duchamp-Viret et al. 1989). This sensitivity improvement may be due to the strong convergence of RNs onto mitral cells or PNs (Schild 1988; Duchamp-Viret et al. 1989; Mori and Shepherd 1994; Laurent 1999). The observed contrast-enhancement of glomerular responses is probably accomplished by inhibitory connections via LNs within the honeybee AL (Sachse and Galizia 2002). As a result of the increased RN input with increasing concentrations, one would expect an amplification of inhibitory inputs to PNs, which should be visible in their glomerular responses. Indeed, glomeruli which were inhibited by a specific odor showed an increased inhibitory response with increasing concentration (Fig. 5A, B). However, we also observed that the total number of inhibited glomeruli decreased again at very high concentrations (Fig. 5C). These two oppositional effects may be due to distinct types of inhibitory input to PNs. We previously proposed a putative glomerular connectivity model which implies two independent inhibitory networks (Sachse and Galizia 2002): a GABAergic inhibitory network effecting an unspecific global gain control mechanism, and a putative histaminergic inhibitory network, which mediates

glomerulus-specific inhibition to contrast-enhance responses of glomeruli with overlapping response profiles. The global, unspecific inhibitory network is effectively invisible at very low concentrations, when only very few glomeruli are getting RN input. At very high stimulus concentrations, it may reduce activity in weak glomeruli, but not push them below resting activity levels. At intermediate levels, however, this network will be sufficiently strong to inhibit not-yet-active glomeruli below base line. The consequence would be our observation in Fig. 5C, where the number of glomeruli inhibited below baseline is maximal at intermediate concentration levels. A corollary of this interpretation would be that inhibitions visible at very low concentrations are due to the glomerulus-specific, putatively histaminergic connections. Further experiments are needed to verify this hypothesis.

Coding properties of odor intensity

Foraging honeybees experienced odors from the same flower at varying concentrations. Behavioral studies have shown that honeybees are capable of generalizing odor quality over a range of concentrations (Bhagavan and Smith 1997; Pelz et al. 1997). Honeybees can also discriminate two concentrations of the same odor differing by a factor of 100 (Vareschi 1971; Kramer 1976; Getz and Smith 1991). An often-stated requirement for odor coding is therefore that odor quality be perceived and possibly processed independently from odor intensity. As a corollary odor quality information should be largely concentration-invariant. Information about odor intensity may be encoded by the overall glomerular activity strength, whereas a concentration-invariant code of odor quality could be realized by different conceivable mechanisms. One strategy could be a read-out of the glomerular order in terms of their relative response intensity. The sequence of active glomeruli in the honeybee AL both at the input and the output side were stable for 1 to 2 log units. However, some glomeruli had steeper response functions than others (Fig. 3, Tab. 1), leading to shifts in the sequence of the most-activated glomeruli and thus substantial changes in the relative activity patterns over a wider concentration range. These findings are in line with several imaging studies of vertebrates (Friedrich and Korsching 1997; Johnson and Leon 2000; Fuss and Korsching 2001; Wachowiak and Cohen 2001; Fried et al. 2002) and invertebrates (Sachse et al. 1999; Galizia et al. 2000), but in contrast to RNs of turtles, whose relative glomerular responses changed only slightly over a concentration range of up to three log units (Wachowiak et al. 2002). It is unclear whether these shifts lead to a shift in perceived odor quality. Thus, if the sequence of glomerular activities encodes odor quality, a concentration-invariance is only apparent for a small intensity range. Our present data suggest a better strategy for intensity-invariance in a manner similar to that used by the visual system, where three types of cones accomplish an intensity-invariant color perception by means of color-opponent encoding. The excitation ratio between the most responsive glomeruli could be the relevant read-out. The ratio between the three strongest glomeruli for the tested odors is shown in Fig. 6A as the direction of the vectors. On the input level this ratio appears

strongly concentration-dependent (Fig. 6Ai), whereas the odor responses of the output neurons revealed an almost concentration-invariant excitation ratio over a concentration range of up to 4 log units due to the glomerulus- and odor-specific contrast-enhancement (Fig. 6Aii). The direction of the vectors is only weakly affected by the different steepness of glomerular response curves. At the same time, the representation of odor intensity is improved due to the continuous increase of the overall excitation in the PNs with increasing concentration. Thus, the AL network optimizes odor representations by separating odor quality information from intensity. Still, psychophysical experiments have to be done to analyze whether the odor quality does indeed persist over the range of concentrations tested to verify the assumptions.

Interestingly, when only the three most sensitive glomeruli are considered, odors at low concentrations are more clearly separated (Fig. 6B). This indicates that the glomerulus-specific contrast-enhancement which emphasizes these most sensitive glomeruli is not perfect and could further be improved by higher processing centers, such as the lateral protocerebrum and the mushroom bodies, by selectively filtering only these responses (i.e. 10%). This raises the question of what mechanism might account for such a selective read-out, if it exists. In locusts the spikes of coactivated PNs are generally synchronized (Laurent et al. 1996; Wehr and Laurent 1996) by the distributed action of GABAergic LNs (MacLeod and Laurent 1996). It is conceivable that PNs from strong glomeruli may synchronize to a stronger extent than those from weaker glomeruli and in this way form the only signal that is read by the mushroom body. In order to investigate this aspect it would be necessary to record from identified glomeruli with high temporal resolution, which is not possible with calcium-sensitive dyes but may be feasible with voltage-sensitive dyes or targeted electrodes.

Taken together, the results show that signal integration within the AL improve a concentration-invariant coding of odor quality, a reliable representation of odor intensity, and odor-identification at low concentrations. Future experiments dedicated to higher order brain centers will help to describe the whole processing path of the olfactory code, ultimately ranging from the RN level to the behavioral response.

ACKNOWLEDGMENTS

We thank Randolf Menzel for helpful discussions and support, Philipp Peele for critical comments on the manuscript, Beate Eisermann for excellent technical assistance and Mary Wurm for help with the English. This work was supported by the Volkswagenstiftung (VW 1/75-399) and HFSP.

REFERENCES

Akers RP and Getz WM. Response of olfactory receptor neurons in honeybees to odorants and their binary mixtures. *J. Comp. Physiol. A* 173: 169-185, 1993.

Bhagavan S and Smith BH. Olfactory conditioning in the honeybee *Apis mellifera*: Effects of odor intensity. *Physiol. Behav.* 61: 107-117, 1997.

Cleland TA and Linster C. Concentration tuning mediated by spare receptor capacity in olfactory sensory neurons: A theoretical study. *Neural Comput.* 11: 1673-1690, 1999.

de Bruyne M, Foster K and Carlson JR. Odor coding in the *Drosophila* antenna. *Neuron* 30: 537-552, 2001.

Duchamp-Viret P, Chaput MA and Duchamp A. Odor response properties of rat olfactory receptor neurons. *Science* 284: 2171-2174, 1999.

Duchamp-Viret P, Duchamp A and Chaput MA. Peripheral odor coding in the rat and frog: Quality and intensity specification. *J. Neurosci.* 20: 2383-2390, 2000.

Duchamp-Viret P, Duchamp A and M. V. Amplifying role of convergence in olfactory system: a comparative study of receptor cell and second-order neuron sensitivities. *J. Neurophysiol.* 61: 1085-1094, 1989.

Duchamp-Viret P, Duchamp A and M. V. Temporal aspects of information processing in the first two stages of the frog olfactory system: influence of stimulus intensity. *Chem. Senses* 15: 349-365, 1990a.

Duchamp-Viret P, Duchamp A and Sicard G. Olfactory discrimination over a wide cocentration range. Comparison of receptor cell and bulb neuron abilities. *Brain Res.* 517: 256-262, 1990b.

Esslen J and Kaissling K-E. Zahl und Verteilung antennaler Sensillen bei der Honigbiene (*Apis mellifera* L.). *Zoomorphol.* 83: 227-251, 1976.

Firestein S, Picco C and Menini A. The relation between stimulus and response in olfactory receptor cells of the tiger salamander. *J. Physiol.* 468: 1-10, 1993.

Flanagan D and Mercer AR. An atlas and 3-D reconstruction of the antennal lobe in the worker honey bee, *Apis mellifera* L. (Hymenoptera: Apidae). *Int. J. Insect Morphol. & Embryol.* 18: 145-159, 1989.

Fried HU, Fuss SH and Korsching SI. Selective imaging of presynaptic activity in the mouse olfactory bulb shows concentration and structure dependence of odor responses in identified glomeruli. *Proc. Natl. Acad. Sci.* 99: 3222-3227, 2002.

Friedrich RW and Korsching SI. Combinatorial and chemotopic odorant coding in the zebrafish olfactory bulb visualized by optical imaging. *Neuron* 18: 737-752, 1997.

Fuss SH and Korsching SI. Odorant feature detection: activity mapping of stucture response relationships in the zebrafish olfactory bulb. *J. Neurosci.* 21: 8396-8407, 2001.

Galizia CG, McIllwrath SL and Menzel R. A digital three-dimensional atlas of the honeybee antennal lobe based on optical sections acquired by confocal microscopy. *Cell Tissue Res.* 295: 383-394, 1999a.

Galizia CG, Nägler K, Hölldobler B and Menzel R. Odour coding is bilaterally symmetrical in the antennal lobe of honeybees (*Apis mellifera*). *Eur. J. Neurosci.* 10: 2964-2974, 1998.

Galizia CG, Sachse S and Mustaparta H. Calcium responses to pheromones and plant odours in the antennal lobe of the male and female moth Heliothis virescens. *J. Comp. Physiol. A* 186: 1049-1063, 2000.

Galizia CG, Sachse S, Rappert A and Menzel R. The glomerular code for odor representation is species specific in the honeybee *Apis mellifera*. *Nat. Neurosci.* 2: 473-478, 1999b.

Gao Q, Yuan B and Chess A. Convergent projections of *Drosophila* olfactory neurons to specific glomeruli in the antennal lobe. *Nat. Neurosci.* 3: 780-785, 2000.

Getz WM and Smith KB. Olfactory perception in honeybees: Concatenated and mixed odorant stimuli, concentration, and exposure effects. *J. Comp. Physiol. A* 169: 215-230, 1991.

Hammer M. The neural basis of associative reward learning in honeybees. *Trends Neurosci.* 20: 245-252, 1997.

Hildebrand JG and Shepherd GM. Mechanisms of olfactory discrimination: Converging evidence for common principles across phyla. *Annu. Rev. Neurosci.* 20: 595-631, 1997.

Joerges J, Küttner A, Galizia CG and Menzel R. Representation of odours and odour mixtures visualized in the honeybee brain. *Nature* 387: 285-288, 1997.

Johnson BA and Leon M. Modular representation of odorants in the glomerular layer of the rat olfactory bulb and the effects of stimulus concentration. *J. Comp. Neurol.* 422: 496-509, 2000.

Kramer E. The orientation of walking honeybees in odour fields with small concentration gradients. *Physiol. Entomol.* 1: 27-37, 1976.

Laurent G. A system perspective on early olfactory coding. *Science* 286: 723-728, 1999.

Laurent G, Wehr M and Davidowitz H. Temporal representation of odors in an olfactory network. *J. Neurosci.* 16: 3837-3747, 1996.

Ma M and Shepherd GM. Functional mosaic organization of mouse olfactory receptor neurons. *Proc. Natl. Acad. Sci.* 97: 12869-12874, 2000.

MacLeod K and Laurent G. Distinct mechanisms for synchronization and temporal patterning of odor-encoding neural assemblies. *Science* 274: 976-979, 1996.

Malnic B, Hirono J, Sato T and Buck LB. Combinatorial receptor codes for odors. *Cell* 96: 713-723, 1999.

Meister M and Bonhoeffer T. Tuning and topography in an odor map on the rat olfactory bulb. *J. Neurosci.* 21: 1351-1360, 2001.

Mombaerts P, Wang F, Dulac C, Chao SK, Nemes A, Mendelsohn M, Edmondson J and Axel R. Visualizing an olfactory sensory map. *Cell* 87: 675-686, 1996.

Mori K and Shepherd GM. Emerging principles of molecular signal processing by mitral/tufted cells in the olfactory bulb. *Sem. Cell. Biol.* 5: 65-74, 1994.

Pelz C, Gerber B and Menzel R. Odorant intensity as a determinant for olfactory conditioning in honeybees: roles in discrimination, overshadowing and memory consolidation. *J. Exp. Biol.* 200: 837-847, 1997.

Ressler KJ, Sullivan KJ and Buck LB. Information coding in the olfactory system: evidence for a stereotyped and highly organized epitope map in the olfactory bulb. *Cell* 79: 1245-1255, 1994.

Rubin BD and Katz LC. Optical imaging of odorant representations in the mammalian olfactory bulb. *Neuron* 23: 499-511, 1999.

Sachse S and Galizia CG. Role of inhibition for temporal and spatial odor representation in olfactory output neurons: a calcium imaging study. *J. Neurophysiol.* 87: 1106-1117, 2002.

Sachse S, Rappert A and Galizia CG. The spatial representation of chemical structures in the antennal lobes of honeybees: steps towards the olfactory code. *Eur. J. Neurosci.* 11: 3970-3982, 1999.

Sato T, Hirono J, Tonoike M and Takebayashi M. Tuning specificities to aliphatic odorants in mouse olfactory receptor neurons and their local distribution. *J. Neurophysiol.* 72: 2980-2989, 1994.

Schild D. Principles of odor coding and a neural network for odor discrimination. *Biophys. J.* 54: 1001-1011, 1988.

Sicard G and Holley A. Receptor cell responses to odorants: Similarities and differences among odorants. *Brain Res.* 292: 283-296, 1984.

Spors H and Grinvald A. Spatio-temporal dynamics of odor representations in the mammalian olfactory bulb. *Neuron* 34: in press, 2002.

Trotier D. Intensity coding in olfactory receptor cells. *Sem. Cell. Biol.* 5: 47-54, 1994.

Uchida N, Takahashi YK, Tanifuji M and Mori K. Odor maps in the mammalian olfactory bulb: domain organization and odorant structural features. *Nat. Neurosci.* 3: 1035-1043, 2000.

Vareschi E. Duftunterscheidung bei der Honigbiene - Einzelzell-Ableitungen und Verhaltensreaktionen. *Z. Vergl. Physiol.* 75: 143-173, 1971.

Vassar R, Chao SK, Sitchran R, Nuñez JM, Vosshall LB and Axel R. Topographic organization of sensory projections to the olfactory bulb. *Cell* 79: 981-991, 1994.

Vosshall LB, Wong AM and Axel R. An olfactory sensory map in the fly brain. *Cell* 102: 147-159, 2000.

Wachowiak M and Cohen LB. Representation of odorants by receptor neuron input to the mouse olfactory bulb. *Neuron* 32: 723-735, 2001.

Wachowiak M, Cohen LB and Zochowski MR. Distributed and concentration-invariant spatial representations of odorants by receptor neuron input to the turtle olfactory bulb. *J. Neurophysiol.* 87: 1035-1045, 2002.

Wehr M and Laurent G. Odour encoding by temporal sequences of firing in oscillating neural assemblies. *Nature* 384: 162-166, 1996.

Witthöft W. Absolute Anzahl und Verteilung der Zellen im Hirn der Honigbiene. *Z. Morph. Tiere* 61: 160-184, 1967.

Yokoi M, Mori K and Nakanishi S. Refinement of odor molecule tuning by dendrodendritic synaptic inhibition in the olfactory bulb. *Proc. Natl. Acad. Sci.* 92: 3371-3375, 1995.